Fusion Engineering and Design 135 (2018) 88–94

Contents lists available at ScienceDirect

Fusion Engineering and Design

journal homepage: www.elsevier.com/locate/fusengdes

Effects of Ti addition on microstructure and mechanical property of spark-plasma-sintered transformable 9Cr-ODS steels

Xiaosheng Zhou, Chong Li*, Liming Yu, Huijun Li, Yongchang Liu*

State Key Lab of Hydraulic Engineering Simulation and Safety, School of Materials Science & Engineering, Tianjin University, Tianjin 300354, PR China

ARTICLE INFO

Keywords:
ODS steels
Ti addition
Oxide nanoparticle
Transformed ferrite
Carbides

ABSTRACT

By adding Ti consistent, dual-phase 9Cr ODS steel with martensite and transformed ferrite is fabricated by spark plasma sintering, and $M_{23}C_6$ carbides are identified in transformed ferrite. Although Ti is strong carbide forming element, Ti concentration has a negligible effect on the distribution of $M_{23}C_6$ within ferrite, as well as martensite size. With Ti addition increasing, the amount of ferrite is increased, and more fine Y-Ti-O complex oxides are produced. Annealing treatment will not change the ferrite distribution, but the density and size of oxide nanoparticles in steels will be affected. It is found that Ti addition can effectively improve the tensile strength of 9Cr ODS steels, which is related to the Y-Ti-O oxides with small size. The large-sized ferrite grains will induce ductile-brittle mixed fracture, deteriorating the ductility of transformable 9Cr ODS steels.

1. Introduction

Oxide dispersion strengthened (ODS) steels have been considered preferentially for structural materials in advanced fission reactors, due to their excellent radiation resistance and high temperature strength [1–4]. These favorable properties originate from the high density of nanoscale oxide particles, dislocations and ultrafine grains [5]. For the past decades, considerable attention has been paid on single phase ferritic ODS steels [6,7]. However, in manufacturing thin-walled tubes, the hot extruded or rolled ferritic steel will suffer from the strength and ductility anisotropies in transverse and longitudinal directions [8–10]. Owing to austenitic and martensitic transformations, martensitic ODS steels can overcome the anisotropy in microstructure and strength. Under the leadership of Professor S. Ukai, ferritic-martensitic dual-phase 9Cr-ODS steels with improved creep strength have been successfully developed. The formation of metastable ferrite (residual ferrite) is related to the pinning force of oxides on α/γ boundaries [11–14].

To produce oxide nanoparticles with smaller size and higher thermal stability, minor alloying elements have usually been added in Y_2O_3-contained ODS steels, like Al, Zr and Ti [15–22]. Ti addition will promote the decomposition of Y_2O_3 in mechanical alloying (MA), and Y-Ti-O complex oxides ranging from 2 to 6 nm will precipitate upon annealing treatment, increasing the number density and volume fraction of nanoparticles and further enhancing high temperature properties [23,24]. On the other hand, the amount of residual ferrite in dual-phase 9Cr-ODS steels can also be tailored by adjusting the concentrations of Ti and excess O (the value obtained by subtracting oxygen concentration coupled with yttrium in Y_2O_3 from total oxygen concentration in steel) [25,26].

Ferritic/martensitic ODS steels are generally fabricated by hot isostatic pressing (HIP) and hot extrusion. Recently, spark plasma sintering (SPS), a field-activated sintering technique, has been prevailing to consolidate ODS-based powders [27–30]. The SPS can produce material rapid densification with fast heating rate, short holding time and low sintering temperature. Thermal exposure of powders, processing times and costs will be reduced, and the nanostructure in milled powders can be retained potentially [31]. In this study, different amounts of Ti are added to the 9Cr martensitic powders, followed by MA and SPS. The effects of Ti addition on microstructure and mechanical property of spark-plasma-sintered ferritic/martensitic 9Cr-ODS steels were investigated in detail.

2. Experimental

Pre-alloyed powders with the nominal composition Fe-9Cr-0.1C-2W-0.2V-0.07Ta (in weight) were produced by inert-gas atomizing, and 0.05 wt.% and 0.1 wt.% Ti element powders were respectively blended with the pre-alloyed powders and 0.35 wt.% Y_2O_3 nanoparticles. The mixed powders were mechanically milled in a planetary ball mill for 45 h, with argon atmosphere as the protection. The rotation speed was 400 rpm, and the ball-to-powder ratio was 15:1. Mechanically milled

* Corresponding authors.
E-mail addresses: lichongme@tju.edu.cn (C. Li), ycliu@tju.edu.cn (Y. Liu).

https://doi.org/10.1016/j.fusengdes.2018.07.019
Received 9 May 2018; Received in revised form 27 June 2018; Accepted 25 July 2018

powders were consolidated with Dr. Sinter SPS-625 machine. Capsuled powders were first heated to 800 °C for 5 min at a rate of ~100 K/min, and then continuously heated to 1100 °C for 10 min with a pressure of 40 MPa, followed by continuous cooling in spark plasma furnace. For martensitic steels, annealing treatment is mandatory to obtain favorable combination of strength and toughness. The SPSed steels were annealed at 800 °C for 1 h under Ar protection.

In this study, the 9Cr-ODS steel containing 0.05 wt.% Ti and 0.1 wt.% Ti is respectively referred as 9Cr-0.05Ti steel and 9Cr-0.1Ti steel. The microstructures of 9Cr-0.05Ti and 9Cr-0.1Ti steels were examined through optical microscopy (OM), scanning electron microscope (SEM) and high resolution transmission electron microscope (HRTEM). For OM and SEM observation, metallographic specimens were etched in a mixed solution of water (100 mL), hydrochloric acid (20 mL) and iron trichloride (5 g). Standard 3 mm TEM discs were ground to a thickness of about 0.07 mm and then thinned by twin-jet electro-polisher with a solution of 5 vol.% perchloric acid in ethanol. Carbon replica technique was also used to analyze the nanoparticle size. After deep etching and carbon coating, the specimen surface was lightly scored into squares of 2.5 mm side length, and then bulk replicas were liberated in the Vilella's reagent, followed by floating the replicas off in 10% methanol/water. Copper TEM grids were used to dry up the replicas. Vickers micro-hardness test was performed with 25 g load and 5 s dwell time. Micro-tensile test was carried out to clarify the effects of Ti addition on mechanical properties of annealed steels, with 10^{-3} s^{-1} tensile rate. The gauge size of plate tensile samples is 5 mm (length) × 1.5 mm (width) × 2 mm (thickness).

3. Results and discussion

3.1. Sintered condition

Fig. 1a and d respectively shows the OM micrograph of sintered 9Cr-0.05Ti and 9Cr-0.1Ti steels. Both of the steels consist of dual-phase structure. The white region represents ferrite phase, while the dark represents the martensite phase. The ferrite exhibits irregular morphologies, and aggregates of ferrite with squeezed morphology can also be readily distinguished, as circled in Fig. 1a and d. Volume fraction of ferrite is evaluated by calculating the area fraction occupied by ferrite. The volume fraction of ferrite in sintered 9Cr-0.05Ti and 9Cr-0.1Ti steels is respectively determined as 16.5 ± 1.5% and 17.9 ± 2.2%. Compared to the microstructure of 9Cr ODS steel without Ti addition [32], it can be seen that Ti addition can promote the formation of ferrite grains in 9Cr ODS steels. The average size of ferrite in sintered 9Cr-0.05Ti and 9Cr-0.1Ti steels is respectively measured as 4.89 ± 3.17 μm and 4.93 ± 3.23 μm. There is no significant effect of Ti concentration on the average size of ferrite phase. It should also be noted that the size of ferrite aggregates in Fig. 1a and d is close to the size of milled powders for 45 h (about 45 μm) [32], which is suggested to be related to the inhomogeneous distribution of Ti in mechanical milling.

Sub-structures of martensite in sintered 9Cr-0.05Ti and 9Cr-0.1Ti steels are shown in Fig. 1b and e. The martensite exhibits block and lath morphologies. In 9Cr-Ti ODS steels, small amount of nano-sized martensite laths can be found, as indicated by the arrow in Fig. 1e. Fig. 1c and f show the ferrite in sintered 9Cr-0.05Ti and 9Cr-0.1Ti steels, respectively. In Fig. 1c, the boundary between martensite and ferrite is not distinct, and it seems that the ferrite gradually grows into martensite. The ferrite/martensite boundary on other parts is not straight, but crooked. Within the ferrite, precipitates of dozens of nanometers are revealed. Based on the selected area diffraction (SAD) pattern, these precipitates are identified as $M_{23}C_6$ carbides. The characteristics of ferrite in 9Cr-0.1Ti steel are similar to those in 9Cr-0.05Ti steel, as shown in Fig. 1f. According to Ukai et al. [33], if the pinning force for α-γ interface boundaries by the oxide particles overcomes the driving force for α→γ transformation, ferrite can be retained at austenitizing temperature, which is designated as the residual ferrite. Oxide nanoparticles with finer size were densely dispersed in the residual ferrite. However, the ferrite in Fig. 1c and f has a low density of dislocations and oxide nanoparticles, and certain amount of $M_{23}C_6$ carbides are identified in ferrite. Considering the high sintering temperature, the $M_{23}C_6$ should be produced in cooling stage instead of heating stage. Since the solubility of carbon in ferrite is smaller than in austenite, the austenite to ferrite transformation may favor the carbide precipitation. Combining with the low density of dislocations and oxide nanoparticles in ferrite, the ferrite shown in 9Cr-Ti ODS steels should be equilibrium ferrite transformed from austenite.

To evaluate the overall oxide size distributions in sintered 9Cr-0.05Ti and 9Cr-0.1Ti steels, carbon replicas are used, as shown in Fig. 2a and b. The average size of oxide nanoparticles in 9Cr-0.05Ti and 9Cr-0.1Ti steels is respectively determined as 9.7 nm and 8.5 nm. In the 9Cr-0.05Ti steel, oxide with the size larger than 20 nm are readily observed, while in the 9Cr-0.1Ti steel, oxides generally have a size smaller than 20 nm. Ti addition can promote the refinement of oxide nanoparticles in 9Cr-ODS steels. Since the oxide size is closely related to its type, it is essential to identify the oxides in Ti-added 9Cr ODS steels. Fig. 3 shows the HRTEM images of different types of oxides in 9Cr-Ti ODS steels, as well as the corresponding FFT images. Cubic Y_2O_3,

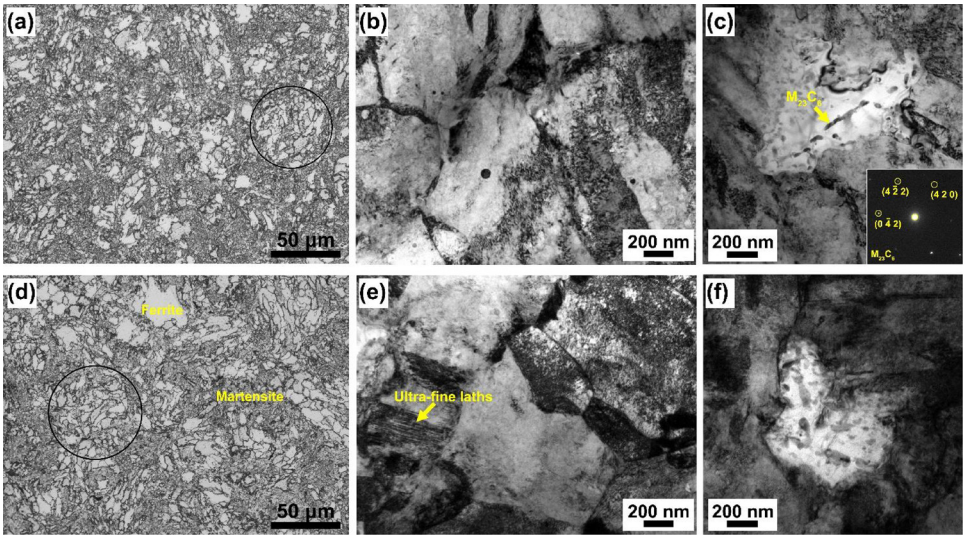

Fig. 1. OM micrographs of (a) 9Cr-0.05Ti and (d) 9Cr-0.1Ti steels and TEM images showing martensite and ferrite in (b), (c) 9Cr-0.05Ti and (e), (f) 9Cr-0.1Ti steels.